Article

Cadmium Removal by Adsorption on Biochars Derived from Wood Industry and Craft Beer Production Wastes

Daiana Simón [1],* , Cristina Palet [2],* and Adrián Cristóbal [1]

1 Instituto de Investigaciones en Ciencia y Tecnología de Materiales (INTEMA), Universidad Nacional de Mar del Plata (UNMdP), Consejo Nacional de Investigaciones Científicas y Técnicas (CONICET), Mar del Plata 7600, Argentina; acristobal@fi.mdp.edu.ar

2 GTS-UAB Research Group, Department of Chemistry, Faculty of Science, Edifici C-Nord, Universitat Autònoma de Barcelona, Carrer dels Til·lers, 08193 Bellaterra, Catalunya, Spain

* Correspondence: dsimon@fi.mdp.edu.ar (D.S.); cristina.palet@uab.cat (C.P.)

Abstract: Cadmium pollution is a serious environmental issue that has an impact on both the ecosystem and human health. As a result, its removal from water is essential. Agro-industrial wastes are suggested as a sustainable adsorbent option, as they are among the most readily available renewable sources worldwide. Biochar is a carbonized biomass that has been shown to be a viable and novel adsorbent. This article compares the results of cadmium adsorption on biochars derived from wood industry and craft beer production wastes. Biochars were characterized before and after adsorption. Batch adsorption results of 0.18 mmol/L Cd(II) concentration solutions indicated adsorption percentages (A%) of 99.7% and 92.2% for sawdust biochar and barley biochar, respectively. For this cadmium concentration, the sawdust biochar presented an adsorption capacity (q_m) of 0.0172 mmol/L, while the barley biochar presented a value of 0.0159 mmol/L. The influence of initial Cd(II) concentration on single and multimetal solutions was studied, and a decrease in Cd(II) adsorption on sawdust biochar was observed in the presence of Ni(II) and Zn(II). The Freundlich isotherm model was found to be the best fit to the data for Cd(II) adsorption isotherms on both biochars. According to the results of this article, sawdust biochar has the best performance as an adsorbent and can be safely disposed of in building bricks at the end of its useful life.

Keywords: barley waste-derived biochar; sawdust waste-derived biochar; cadmium adsorption; multimetal solution; circular economy; spent adsorbents

1. Introduction

Water contamination by toxic heavy metals is a serious environmental issue that society, industry, and public authorities are concerned about [1]. Cadmium (Cd) enters the environment through geogenic processes such as rock weathering, soil particles, volcanic eruptions, forest fires, and sea salt, as well as anthropogenic processes such as fossil fuel combustion; battery, pigment, and fertilizer manufacturing; iron, steel, and cement production; mining; and PVC product stabilization, among others that have contributed to its wide dispersal in the environment [2]. Cd is relatively nonbiodegradable and is one of the most toxic, bioaccumulative, and mobile heavy metals in the environment and has no recognized physiological function [3,4]. It is classified as a hazardous and priority pollutant because exposure to it through water contamination causes kidney and liver dysfunction; bone, testicular, adrenal gland, and hematopoietic system damage; neurological disorders; pulmonary edema and chronic itai-itai disease, and the International Agency for Research on Cancer (IARC) classifies it as a human carcinogen (group I) [5,6]. As a result, the US Environmental Protection Agency (USEPA) [7] and the Argentine Food Code (CAA) [8] established a maximum cadmium level in drinking water of 0.005 mg/L.

Protecting the environment and human health is one of the challenges that humanity faces in order to ensure sustainable development and environmental safety. Three of the

most used conventional technologies for removing/recovering cadmium from wastewater include membrane separation, ion exchange, and chemical precipitation. Unfortunately, these treatments may be expensive in terms of both operation and materials, and they can also produce a lot of sludge [6,9]. Adsorption is a surface phenomenon that involves mass transfer between a liquid (or gas) phase containing the adsorbate and a solid phase containing active adsorption sites via weak physical or Van der Waals forces (physisorption) or strong chemical forces via covalent bonds (chemisorption) [10]. Adsorption has been promoted as a cost-effective, efficient, and simple-to-use technology in recent years; nevertheless, the optimal adsorbent (inexpensive, large surface area, high adsorption capacity, mechanical stability, and the ability to be easily regenerated) has yet to be developed [1,11]. Factors such as pH, temperature, ionic strength, contact time, initial adsorbate concentration, and adsorbent dosage influence the interaction between adsorbent and contaminant and hence the efficiency of the adsorption process [12].

Several industries use activated carbon as an adsorbent, but its main disadvantage is its high production and regeneration cost [4,13]. Agro-industrial waste accounts for a significant portion of solid waste, and its management is a challenge in developing countries due to the high cost of effective treatment [9]. The reuse of these wastes gives them economic value and serves as an incentive for the agro-industrial sector [14]. Because these wastes are inexhaustible, inexpensive, and locally available, they have been studied as Cd(II) adsorbents; such is the case of banana peels [15], husks of lentils [16], eggshell powder [17], and peanut shells [18], among others. The presence of binding groups on the surfaces of these materials, such as ether, carbonyl, and hydroxyl, contributes to their affinity and selectivity for cadmium and other heavy metals [19].

Another alternative for the reuse or management of agro-industrial waste is to produce biochar, which is a carbonized form of biomass produced under oxygen-limited conditions and moderate temperatures (700 °C) [20,21]. This material has recently been proposed as an adsorbent material for the removal of heavy metals due to its great effectiveness and the fact that it does not require advanced activation methods [22]. The structure of biochar is distinguished from activated carbon by the absence of activation and by carbonized and noncarbonized fractions with micro-, meso-, and macropores, a large surface area, and the presence of oxygen functional groups and minerals, which improves its performance as an adsorbent in comparison to its biomass of origin [23–25].

The aim of this study was to compare the adsorption of Cd(II) on two biochars derived from two different raw materials: sawdust (SB) and barley (BB), the wastes coming from the wood industry and craft beer production, respectively. South America is becoming an important producer in the global forest sector, supplying raw materials from conifers such as pine that are relevant to sawmills. In Argentina, sawdust accounts for up to 15% of the biomass discarded by sawmills [26]. Craft beer production, for its part, has expanded throughout Argentina over the last 20 years, with barley residue being one of the most abundant residues generated by the food industry [27]. Therefore, proper management of sawdust and barley wastes is of increasing concern due to their negative ecological and economic impact. The research motivation was to use biochar, characterized by a high adsorption capacity, produced by these two key industrial sectors (wood industry and craft beer production) from cheap and readily available feedstock biomass, such as sawdust and barley wastes. Biochars may have varying characteristics depending on the feedstock and preparation conditions, which could impact their efficacy as adsorbents [23]. This study might contribute to further advance the application of biochars in the removal of cadmium from contaminated aqueous systems, thus promoting the concept of the circular economy and guaranteeing the safe disposal of spent adsorbents (secondary contaminants). The specific objectives proposed were to thoroughly characterize the biochars investigated as adsorbents, to compare Cd(II) adsorption to that of other heavy metals of environmental concern, to investigate the influence of adsorbate concentration on cadmium ion adsorption in single- and multimetal systems (important before implementing this technology), to

evaluate Cd(II) adsorption isotherms in the two biochars, and finally, to check the safe final disposal of biochars spent in the production of building bricks.

2. Materials and Methods

2.1. Biochar Characterization

Biochar derived from pine sawdust (SB) was provided by a sawmill in northern Argentina in Corrientes Province (northeast region of Argentina). Barley biochar (BB) was provided by a craft beer SME (small and medium-sized enterprise) in the province of Buenos Aires (central-eastern region of Argentina). Both biochars were produced by the factories in their respective locations in order to reduce the volume of their discards. The biomasses were carbonized in boilers at an uncontrolled temperature to avoid the release of large amounts of carbon dioxide as an environmental pollutant. Therefore, these biochars correspond to real waste that the respective industries want to dispose of. The biochars were then processed in the laboratory to a particle size of 710 μm or less.

Brunauer–Emmett–Teller (BET) analysis (Micromeritics-FlowSorb II 2300 (Norcross, Georgia)) was used to estimate textural properties, such as surface area of the biochar, that affect the interaction of the adsorbate with the adsorbent and to give information for the assessment of the sites available for adsorption. The equipment was calibrated with an alumina standard, injecting 1 cm^3 of pure N_2, which gave a surface area of 2.84 m^2. The sample was dried at 100 °C, and after introducing it into the equipment, a pretreatment at 250 °C was carried out. The morphology, crystalline structure, elemental analysis, and surface chemistry composition of the biochars were determined by using different techniques, such as scanning electron microscopy (SEM) and energy-dispersive X-ray spectroscopy (EDS) (Zeiss Crossbeam 350 Field Emission Scanning Electron Microscope with EDS/EBSD/FIB with maximum magnification of 100.000× (Oberkochen, Germany)); X-ray diffraction (XRD) (PANalytical X'Pert PRO equipment, with Cu K-alpha radiation = 1.5406 nm in operating conditions of 40 kV and 40 mA (Almelo, The Netherlands)) using HighScore Plus software (Version 2.2d (2.2.4)) and the International Center for Diffraction Data X-ray powder diffraction pattern database; attenuated total reflectance–Fourier transform infrared spectroscopy (ATR-FTIR) of powder samples (Nicolet 6700, Thermo Electron Corp. equipment, Waltham, MA, USA, operating in the spectral range of 4000–400 cm^{-1}); and X-ray fluorescence (XRF) (PW4024 Minipal 2 PANalytical X-ray spectrometer with copper anode in operating conditions of nitrogen flow, voltage 20 kV, current 5 mA, and time 100 s (Almelo, The Netherlands)). Furthermore, the adsorbent's thermal stability was evaluated using differential thermal analysis (DTA) and thermogravimetric analysis (TGA) (Shimadzu TGA-50 and Shimadzu DTA-50 instruments, respectively, with TA-50 WSI analyzer in operating conditions of air, heating rate of 10 °C/min to 1000 °C, and approximately 20 mg of mass (Kyoto, Japan)). In addition, point of zero charge (PZC) and pH (pH meter ADWA AD1000 (Szeged, Hungary)) and electrical conductivity (Hach Sension 378 Laboratory Multiparameter Meter (Loveland, CO, USA)) were also analyzed for the characterization of surface chemistry and physicochemical properties of biochars. PZC describes the electrical state of an adsorbent's surface in solution and was determined by adding 0.5 g of biochar to 50 mL of distilled water with a pH between 3 and 11 units (adjusted with appropriate amounts of HCl 0.1 mol/L and NaOH 0.1 mol/L). The final pH value was measured after 24 h under agitation. The PZC is the point at which the final pH–initial pH curve as a function of initial pH cuts the *x* axis. pH and conductivity were determined after 1 g of sample was mixed with 10 mL of deionized water for 90 min.

2.2. Chemicals and Reagents

Stock solutions of Ni(II), Zn(II), and Cd(II) at 1000 mg/L concentration were prepared by dissolving the required weighted amounts of $Ni(NO_3)_2 \cdot 6H_2O$, $Zn(NO_3)_2 \cdot 6H_2O$, and $Cd(NO_3)_2 \cdot 4H_2O$ (Panreac, Spain, analytical reagent grade). Direct dilution of the stock solutions was used to prepare all of the solutions with known initial concentrations utilized in the adsorption testing. Hydrochloric acid (HCl) and sodium hydroxide (NaOH) were

used at 0.1 mol/L (Panreac, Spain, analytical reagent grade). The MilliQ water system was used (Millipore, Billerica, MA, USA).

2.3. Batch Adsorption Experiments

2.3.1. Adsorption of Cd(II) and Other Heavy Metals

Each one of the metal stock solutions was diluted to a concentration of 0.18 mmol/L. The pH of the diluted solutions was adjusted between 4.0 and 5.0. The pH of the solution can influence heavy metal adsorption. For example, when the pH is less than 7.0, cadmium ions predominate, but when the pH is higher than 8.0, Cd(II) can precipitate as cadmium hydroxide [22]. Because the high concentration of hydronium ions in solution causes a large competitive mechanism with cadmium ions and protonates the functional groups by positively charging the adsorbent surface, low pH values have a negative effect on cadmium adsorption [28]. As a result, solutions at room temperature and with a mildly acidic pH are appropriate for interacting with the target heavy metal ions. A 10 mL volume of the heavy metal solution was mixed with 100 mg of biochar. A rotary shaker (CE 2000 ABT-4, SBS Instruments SA, Barcelona, Spain) was used to mix the system at a speed of 40 rpm. The adsorption experiment was completed within 24 h to ensure that the contact between adsorbate and adsorbent was sufficient to achieve equilibrium. Finally, the liquid phase was filtered using 0.22 μm Millex-GS Millipore filters (from Jasco, Tokyo, Japan), and the metal concentration in the aqueous final solution was determined using inductively coupled plasma–mass spectrometry (ICP-MS) (XSERIES 2 ICP-MS, Thermo Scientific, USA) from the Autonomous University of Barcelona. All samples were prepared in duplicate, and adsorbed heavy metal amount was calculated by using Equations (1) and (2) [29]:

$$A\% = \frac{(C_0 - C_e)}{C_0} \times 100 \tag{1}$$

$$q_e = \frac{(C_0 - C_e) \times V}{m} \tag{2}$$

where $A\%$ (%) is the adsorption percentage, q_e (mmol/g) is the adsorbent's adsorption capacity, C_0 and C_e (mmol/L) are the initial and equilibrium heavy metal concentrations in solution, V (L) is the volume of the heavy metal solution, and m (g) is the used weight of the adsorbent.

2.3.2. Effect of Initial Cd(II) Concentration in Single- and Multi-Metal Systems

The effect of the initial concentration of contaminant on its adsorption process was determined by changing it in the aqueous solution in a proper range. Typically, the initial adsorbate concentration ranges between 0 and 500 mg/L [22]. Using the aforesaid protocol in the single system, an initial Cd(II) concentration was varied from 0.05 to 4 mmol/L (6 to 450 mg/L) to evaluate the effect of initial concentration on cadmium adsorption. The same concentration range was used for Cd(II) in the mixed or multimetal solution containing Zn(II), Ni(II), and Cd(II) (closer to a typical effluent, where heavy metals are rarely encountered alone). Both set of results were properly compared.

2.3.3. Adsorption Isotherms

The adsorption of cadmium in single-metallic solutions was mathematically modelled by adjusting the adsorption equilibrium data in terms of isotherm models. To represent the interaction mechanism between contaminants and adsorbents, the Freundlich and Langmuir isotherm models are the most commonly used for their simplicity and easy interpretation [29–32].

The Langmuir model assumes that adsorption occurs on a finite number of homogenous sites per monolayer, with no interaction between adsorbate molecules. The model is described mathematically by Equation (3), where q_m (mmol/g) is the maximum saturated monolayer adsorption capacity of an adsorbent, and K_L (L/mmol) is the Langmuir equilib-

rium constant showing affinity for the active site and is related to the heat of adsorption and free energy. The adsorption system's separation factor or equilibrium parameter (R_L) is a dimensionless constant that can predict the shape of the equilibrium isotherm curve and can be determined using Equation (4).

$$q_e = \frac{q_m \times k_L \times C_e}{1 + K_L \times C_e} \tag{3}$$

$$R_L = \frac{1}{1 + K_L \times C_0} \tag{4}$$

The Freundlich model takes into account adsorption's nonideality and reversibility. Adsorption occurs on a heterogeneous surface with unequal adsorption sites and different adsorption energies, according to this concept, through multilayering and interaction of the adsorbed molecules with each other. Equation (5) is a mathematical equation that describes the Freundlich model, where K_F ($mmol^{1-(1/n)}\ L^{1/n}\ g^{-1}$) is the Freundlich equilibrium constant related to adsorbent capacity and n (dimensionless) is the Freundlich intensity parameter and allows one to predict the shape of the isotherm.

$$q_e = K_F \times C_e^{\frac{1}{n}} \tag{5}$$

A nonlinear regression approach was used to estimate the parameters of the isotherm models, which have a nonlinear shape. In this method, the bias between the q_e values determined from the experimental data and those estimated from the models may be reduced. Origin Pro 9.1 was used to compute the parameters of the nonlinear Langmuir and Freundlich isotherm models. The correlation coefficient (R^2) of each model was determined, considering that the chi-square value was closest to zero, to examine the suitability of the model when fitting the adsorption data [29].

2.4. Clean Disposal of Spent Biochars

Sawdust biochar (SB) spent was used in the manufacture of fired clay bricks as a pore-forming agent. The preparation of these bricks is detailed by the authors in a previous work [33]. Biochar was added to the clay at a ratio of 20% by volume to the volume of mineral. Six percent of water was added to the mixture, and bricks were formed in 70 mm × 40 mm × 18 mm molds by uniaxial compression at a pressure of 25 MPa. After 24 h of air drying, the bricks were fired at 950 °C using a standard ceramic industry firing curve. For more details on the tests performed on these bricks (and other ones prepared with other spent lignocellulosic adsorbents), refer to previous works [33,34]. In the present investigation, leaching tests were carried out on bricks prepared from spent SB. For this purpose, EPA method 1311 [35], a procedure recognized by Argentine laws for hazardous waste, was used as a basis, with an extraction aqueous medium at pH 4.93 ± 0.05 and with pulverized brick samples. In addition, the pollutant retention efficiencies of the brick samples were calculated from the mass of heavy metal in the leachate and the estimated initial mass of contaminant in the brick [36].

3. Results and Discussions

3.1. Biochar Characterization

The nature of the adsorbent determines many of its physical and chemical characteristics that play a crucial role in its performance as an adsorbent. To fully comprehend how adsorption of the contaminant occurs, the adsorbent must be extensively characterized before and after the adsorption process.

Table 1 summarizes some physicochemical properties of the characteristics of sawdust and barley biochars (SB and BB, respectively). It has been demonstrated that thermal degradation of plant feedstock increases the pore volume of biochars in comparison to the biomasses. Because pore volume and surface area are strongly associated, the increase in surface area in biochar can be attributed to pore size distribution [24]. Table 1 shows that

SB presented a higher BET surface area value compared to BB. Higher surface area and thus larger pore volume could enhance the adsorption of contaminants because metal ions could physically adsorb on the surface and be retained within the biochar pores [37,38]. Because PZC indicates solution conditions with zero surface-charge density, the biochar surface is negatively charged for pH values above PZC and positively charged for pH values below PZC. A higher negative surface charge favors electrostatic interactions and consequently the adsorption of Cd(II) ions [30,39]. According to the PZC results obtained for SB and BB biochars (10.25 and 7.24, respectively), electrostatic interactions might not play a predominant role in Cd(II) adsorption since both biochars presented a positive surface charge (PZC) at working pH (4.0–5.0) [40]. The high electrical conductivity of SB (1606 $\pm$ 20 μs/cm at 25 °C) with respect to BB (361.11 $\pm$ 11 μs/cm at 25 °C) suggests a considerable concentration of soluble salts on its surface. In addition, SB presented a higher basicity than BB (pH equal to 10.02 $\pm$ 0.02 and 6.80 $\pm$ 0.01, respectively), which could result in a higher adsorption efficiency of heavy metals because they can also precipitate on the biochar surface [41,42].

Table 1. Physicochemical properties of SB and BB.

Biochar	BET Surface (m²/g)	PZC	pH	Conductivity (μs/cm)
SB	320	10.3	10.02 $\pm$ 0.02	1606 $\pm$ 20
BB	66	7.2	6.80 $\pm$ 0.01	361 $\pm$ 11

SEM images of SB and BB biochars prior to cadmium adsorption are shown in Figure 1A and 1B, respectively. SEM images of both biochars show some of the micromorphology of the starting biomass. It is noted that SB has a flat microstructure, while BB appears to have a rougher surface. The porous structure of both biochars was due to volatilization of organic materials during pyrolysis and could favor the adsorption of Cd(II) [21]. In addition, there were no observable changes in the micromorphology of the adsorbents caused by cadmium ion interaction after adsorption (Figures 1C and 1D, respectively). Figure 1 also shows X-ray elemental mapping confirming a homogenous spatial distribution of cadmium in both biochars (Figures 1C and 1D). The elemental composition of SB and BB before and after Cd(II) adsorption obtained by EDS is presented in Table 2. Semiquantitative elemental analysis indicated that both biochars had substantial levels of carbon and oxygen. Otieno et al. 2021 [43] observed similar results with pineapple peel biochar. The presence of 0.7% and 0.3% of Cd on SB and BB, respectively, verified the adsorption of these metal ions on both adsorbents.

The diffraction analysis of these adsorbents is presented in Figure 2 and shows the presence of semicrystalline cellulose as an organic component, with a broad peak centered at 25 degrees [44–46]. The amorphous phases of the sawdust and barley (SB and BB, respectively) components were eliminated by heat treatment of the biomass feedstocks. However, a significant amount of amorphous phase is observed to be present, especially in BB. There is a decrease in intensity and an increase in amorphous peak width in SB with respect to BB, which allowed the identification of peaks corresponding to SiO_2 in quartz structure, $CaCO_3$ in calcite structure, MgO in periclase structure, Fe_2O_3 in maghemite structure, and graphite. According to Inyang 2015 [42], during the preparation of a biochar, the amounts of Ca, Mg, Fe, and Si, among other elements, are increased, which could favor adsorption via surface precipitation via the interaction of metal ions with mineral phases.

Figure 3 shows the FTIR spectra of SB and BB. Although there are discrepancies between functional groups identified in both biochars due to raw material and processing conditions, the presence of oxygen functional groups (C=O, COO-, and OH-) and aromatic carbon groups could enhance cadmium ion binding via complexation processes [21,37,38,43,46,47]. Because the feedstock for both biochars, sawdust (SB) and barley (BB), are mostly constituted of cellulose and lignin, the FTIR spectra of both biochars demonstrate the presence of aromatic carbonyl and acid–carboxyl groups, with C=O stretching at 1726 and 1699 cm^{-1} (SB and BB, respectively). The bands at 2974–2980 cm^{-1} and

2885–2889 cm^{-1} correspond to the C-H stretching of the -CH$_2$ and -CH$_3$ groups of long-chain aliphatic compounds in SB and BB biopolymers. The band observed at 1562 cm^{-1} exclusively in barley biochar is associated with the -COO stretching of acids containing the carbonyl group and the C=C skeletal vibrations of aromatic compounds. The bands at 1419 and 1387 cm^{-1} in BB and SB, respectively, were assigned to C-H deformation in the alkanes, cycloalkanes, and alkyl group; C-O stretching and O-H deformation (in plane) of tertiary alcohols and phenols; and C-O stretching and O-H deformation of acids containing the carbonyl group. A band between 1263 to 1230 cm^{-1} was identified in these biochars and was assigned to the stretching of aromatic CO- and phenolic -OH. The large band in both biochars at about 1080–1047 cm^{-1} corresponds to aliphatic ethers (C-O-C) and alcohols found in cellulose. Aromatic ring C-H bending is in the region corresponding to the 879, 872, and 748 cm^{-1} bands. The band at 669 cm^{-1} is related to the phenyl vibration. According to López et al., 2020 [23], the well-marked narrow band in SB at 872 cm^{-1} may be attributed to the presence of carbonates in this biochar that could enhance cadmium surface precipitation adsorption. Therefore, discrepancies between the functional groups identified in the biochars could explain the differences in cadmium adsorption on SB and BB.
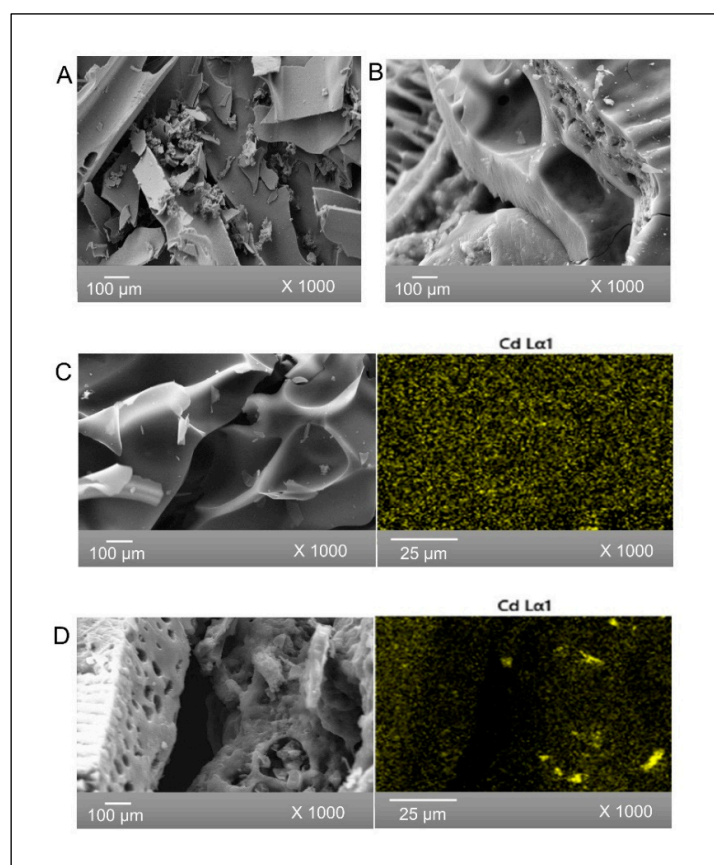

Figure 1. SEM images of (**A**) SB and (**B**) BB, both before Cd adsorption, and (**C**) SB and (**D**) BB, both after Cd(II) adsorption, together with X-ray cadmium mapping.

Table 2. EDS semiquantitative elemental analysis of the biochars before and after Cd(II) adsorption.

Element	Weight (%)			
	SB before	**SB after**	**BB before**	**BB after**
C	72.3	76.1	72.3	62.6
O	23.1	19.8	24.4	29.5
Ca	2.1	1.7	0.5	0.9
K	1.1	0.5	0.2	0.3
Mg	0.4	0.4	0.7	0.9
Si	0.3	0.1	0.1	3.7
Cl	0.2	-	-	-
S	0.2	-	0.1	-
Al	0.1	-	-	-
P	0.1	-	1.4	1.9
Na	-	-	0.5	-
Mn	-	0.8	-	-
Cd	-	0.7	-	0.3
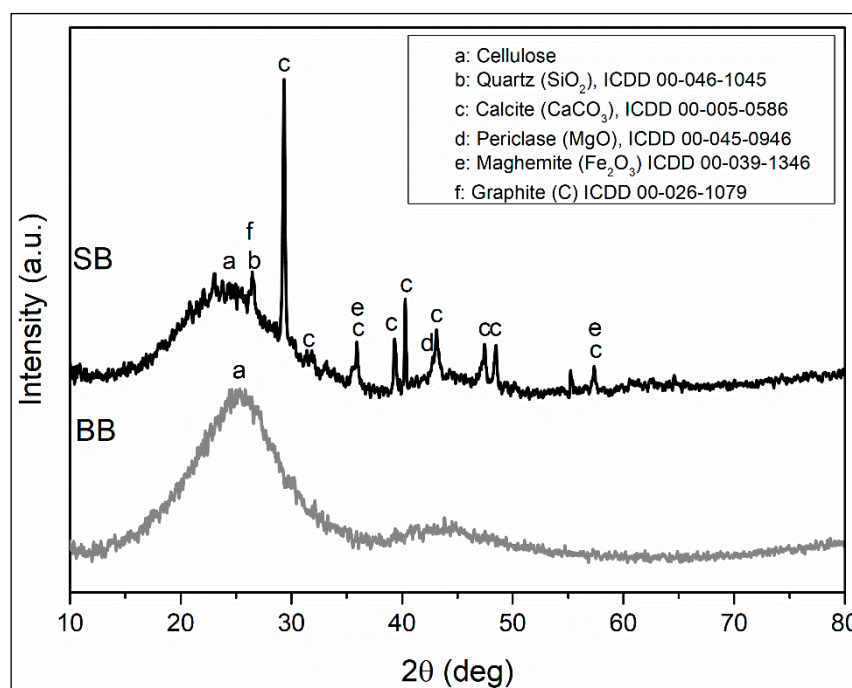
Figure 2. XRD patterns of biochars.

XRF analysis of the biochars, as observed in Figure 4, revealed the inorganic content of SB and BB samples. Because the equipment used cannot measure elements lighter than Na, the presence of H, C, and O is not detected. The Cr peaks were caused by the tube used as the source of the equipment (anode). Biochars are rich in the inorganic portion of the feedstock (sawdust and barley) that is not volatilized during pyrolysis [23]. It should be mentioned that the mineral portion of the biomass is composed of K, Ca, Mg, and P and is preconcentrated during pyrolysis due to ash formation, probably contributing to favor the adsorption of cadmium ions by ion exchange [41,42]. In addition, Figure 4 shows the peaks corresponding to the presence of adsorbed Cd in both biochars, lines 3 to 3.5 keV (Cd Lα, Cd Lβ1, and Cd Lβ2).
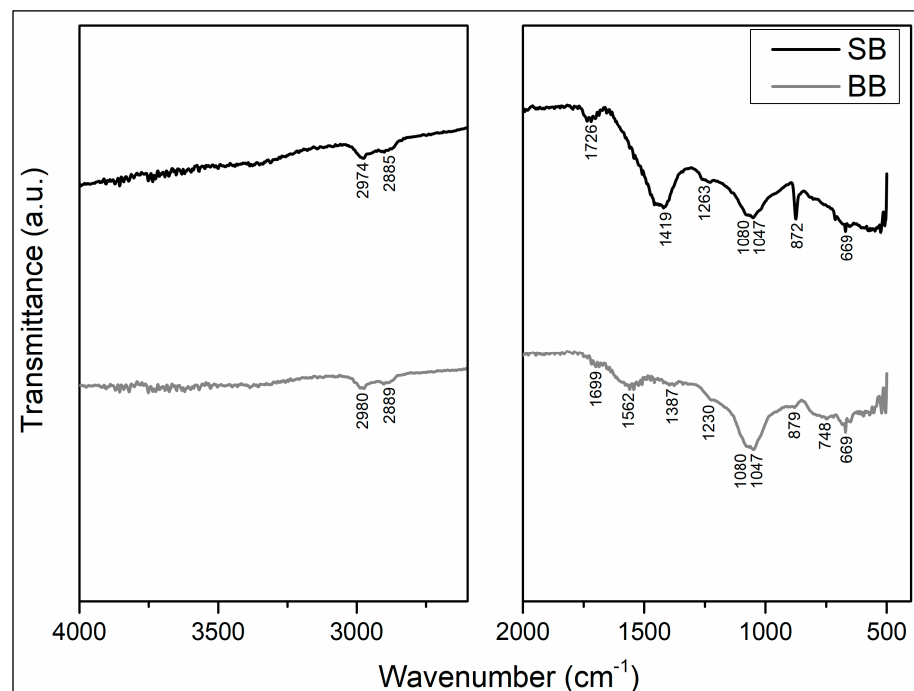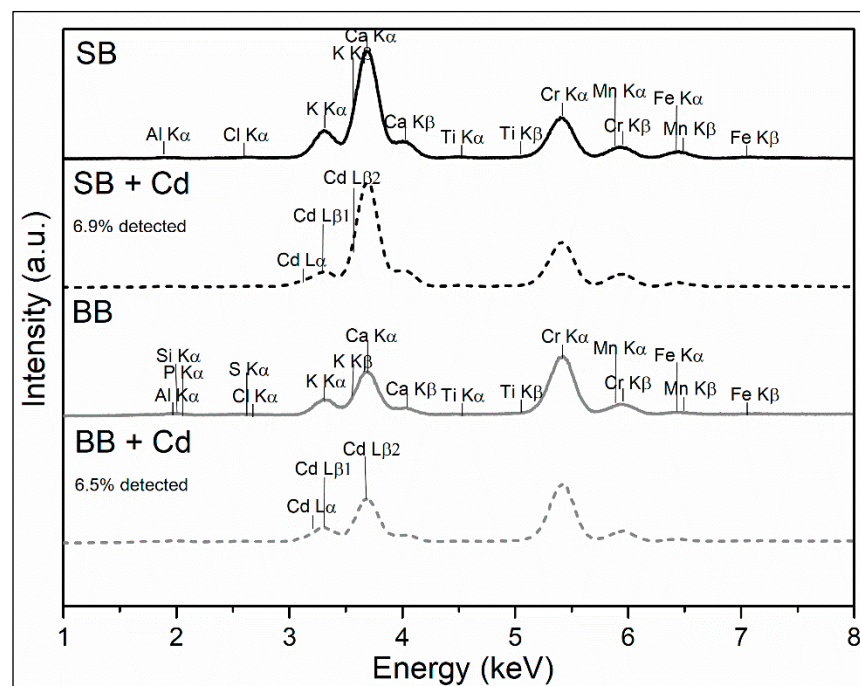
Figure 3. Biochars ATR-FTIR spectra.

Figure 4. XRF analysis of biochars.

The TGA-DTA tests of the two biochars are presented in Figure 5. The large mass loss observed indicates that the adsorbents maintained part of the original plant structure. The TGA-DTA analysis reveals the following thermal phenomena that are consistent with the literature [43,46,48]:

- Sample moisture loss (endothermic peak at 50 °C, SB). This event marks the first stage in losing weight of 7% (up to 115 °C) in SB and BB.
- Decomposition of cellulose and, primarily, lignin into CO_2, H_2O, and ash (exothermic peak at 430 °C and 488 °C SB and BB, respectively), indicated by a second stage

of weight loss of 50% and 79% SB and BB, respectively (up to 470 °C SB and up to 550 °C).

- A small final weight loss of 5% and 3% that might be related to CO_2 evolution (carbonate decomposition).
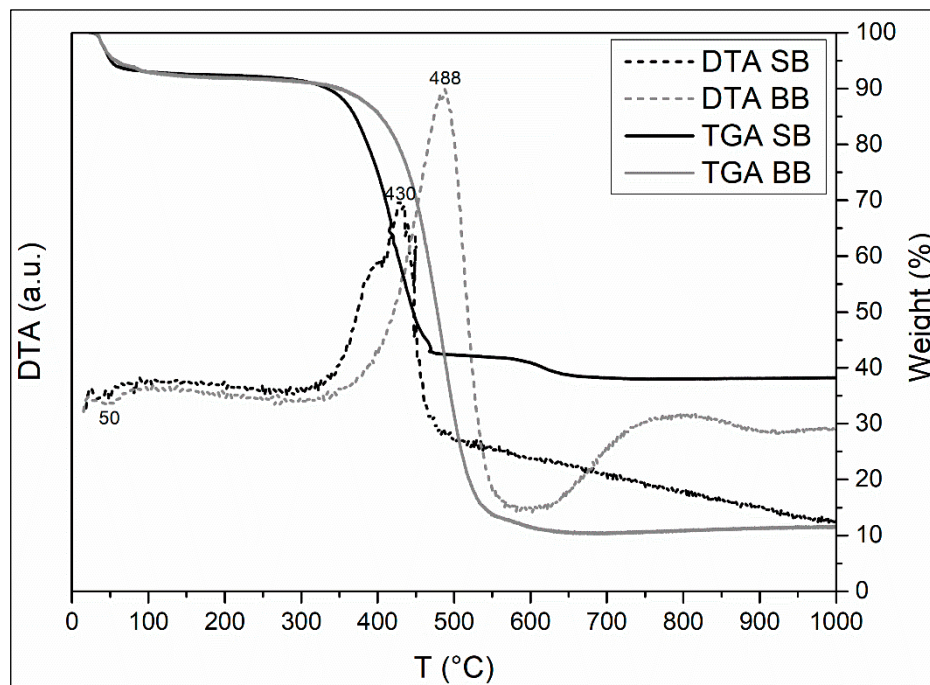

Figure 5. TGA-DTA curves of biochars.

Due to the larger number of volatile chemicals, TGA analysis shows that their thermal decomposition at lower temperatures is higher in the sample of SB than in the sample of BB. Finally, the TGA analysis reveals that there is greater inorganic material in SB as measured by the quantity of remaining mass at the finish of the calcination (SB: 38% and BB: 11%). These results are consistent with the higher pH value for SB compared to BB, which could be attributed to the decomposition of organic components into alkaline salts [48]. As previously stated, the ash and inorganic components could bind heavy metals and promote their adsorption by cation exchange [42].

3.2. Batch Adsorption Experiments

Figure 6 shows the results of the adsorption tests according to the values of adsorption percentage (*A*%) and adsorption capacity (*q_e*). For both adsorbents, the adsorption percentages of Cd(II) at the initial concentration of 0.18 mmol/L were close to and greater than 90%. In addition to Cd(II), two additional metal ions, Zn(II) and Ni(II), were selected to evaluate and compare the performance of each biochar as adsorbents also for these toxic heavy metals. According to the results, the yields of both biochars varied, with sawdust biochar (SB) being superior to barley biochar (BB). This is consistent with the characterizations of both adsorbents depicted and discussed in Section 3.1, which emphasize the influence of processing and feedstock variables on the performance of biochar as an adsorbent. Ni(II) showed the lowest adsorption on BB (Figure 6A), which could be explained by the hydration energy value. This cation has a higher hydration energy than zinc and cadmium cations (Ni(II): −2106 KJ/mol, Zn(II): −2044 KJ/mol, and Cd(II): −1806 KJ/mol) and therefore less capacity to lose water molecules from its coordination sphere, keeping it from being strongly retained by the adsorbent [37]. On the other hand, the higher porosity and mineral content in SB determined an increase in Ni(II) adsorption possibly due to its smaller ionic and hydration radius (Ni(II): 4.04 Å, Zn(II): 4.30 Å, and Cd(II): 4.26 Å), which would facilitate greater penetration into the biochar pores and favor adsorption by ion

exchange [42,49]. The adsorption is controlled by a trade-off between penetration (small hydrated ionic radius) and interaction (smaller hydration energy) of heavy metals with respect to the adsorbent, according to Petrella et al., 2018 [50]. In addition, from the analysis to characterize both materials, it was found that the initial pH of the aqueous solutions containing the heavy metals to be adsorbed is not an important factor in their adsorption performance. Furthermore, as mentioned previously, the surface pH and the site groups are two characteristics of biochars that can provide an environment favorable to the metal surface precipitation on the sorbent surface [51].
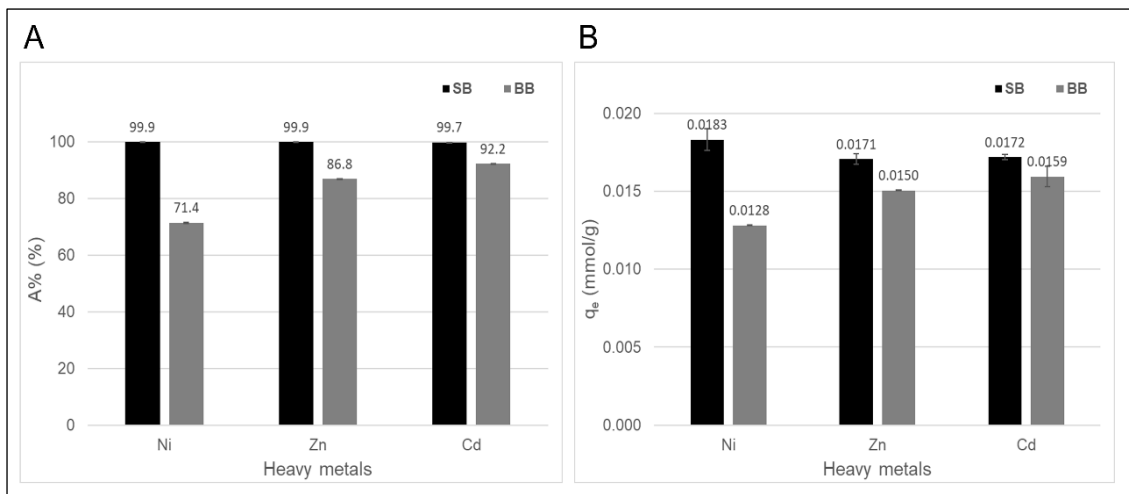

Figure 6. (**A**) Adsorption percentage (*A*%) and (**B**) adsorption capacity (q_e) of aqueous Ni(II), Zn(II), and Cd(II) solutions on both biochars. Initial metal concentration of 0.18 mmol of each metal, contact time of 24 h, initial pH of 4.0–5.0, and 100 mg of adsorbent in 10 mL of initial solution. The tests were performed in duplicate, and the average values are reported with their respective error values.

The influence of the initial Cd(II) concentration on its adsorption by using both biochar adsorbents, either in single- or multielement solutions, is shown in Figure 7. As it can be seen from results collected in Figure 7A, as the initial concentration (C_0) increases, the *A*% decreases, probably because of the saturation of adsorption active sites that are limited in the adsorbents [52,53]. On the other hand, the adsorption capacity increases as the initial adsorbate concentration increases, as can be seen in Figure 7B. This is attributed to an increase in adsorption rate caused by greater collisions between metal ions and the adsorbent, as well as metal diffusion to the biochar's surface and pores [45,54]. However, for high initial cadmium concentrations, a tendency to reach a plateau is observed, because adding more metal cannot increase adsorption due to the saturation of the material [32].

Most of the papers on adsorption in agro-industrial wastes focus on the removal of Cd(II) from aqueous solutions by single-metal systems. However, in multimetal systems, closer to real effluents, there is competition for adsorption sites, which could lead to alterations in the adsorption process of the cadmium ions, especially at high concentration levels [12]. Figure 7 shows the variation in adsorption percentage and adsorption capacity of Cd(II) as a function of initial metal concentration in a multimetal solution with Ni(II), Zn(II), and Cd(II). When SB was used as an adsorbent, the adsorption of cadmium with an increase in its initial concentration was found to be lower in the multimetal solution than in the single-metal solution. The fact that a fixed amount of adsorbent has a finite number of binding sites explains this behavior [48,55]. And there is an excess of active sites on the biochar adsorbents at low initial metal concentrations; therefore, competition between heavy metals increases at relatively high concentration levels [32,38]. The aforementioned behavior is not seen when barley biochar (BB) was used as the adsorbent, indicating the differences in its composition and structure.
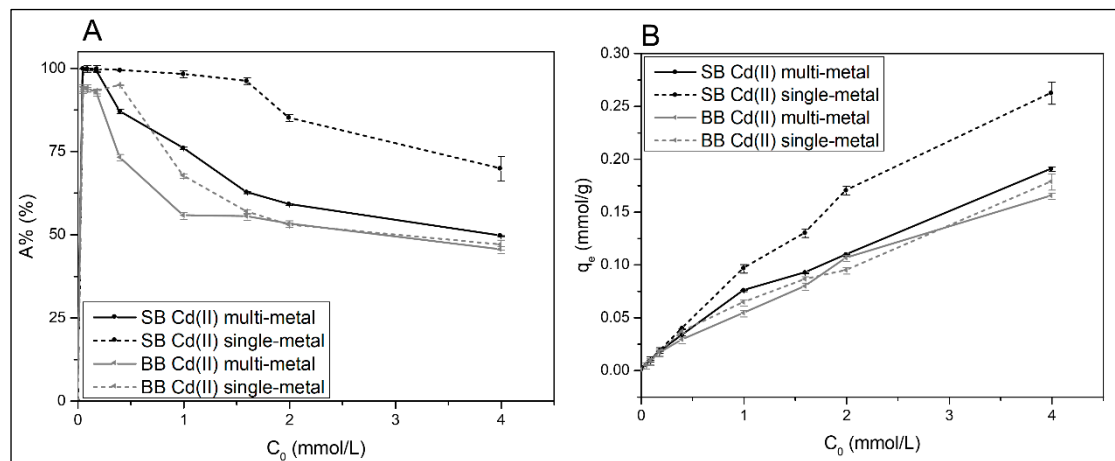
Figure 7. (**A**) Adsorption percentage (*A*%) and (**B**) adsorption capacity (q_e) of Cd(II) as a function of initial concentration (C_0) on both biochars. Contact time of 24 h, initial pH of 4.0–5.0, and 100 mg of adsorbent in 10 mL of initial solution. The tests were performed in duplicate, and the average values are reported with their respective error values.

Figure 8 shows the adsorption isotherms of Cd(II) in a single-metal solution on SB and BB as a function of the metal concentration in the equilibrium (C_e). At adsorption equilibrium, the amount of Cd(II) adsorbed on the solid phase (q_e) increases substantially with the metal concentration present in the aqueous solution (C_e) at low C_e. This behavior becomes less substantial as C_e increases, most likely due to saturation of the adsorbent [56]. Table 3 summarize the parameters derived from the Langmuir and Freundlich isotherm models, as well as the data correlation coefficient (R^2). Although the chi-square value was considered as close as possible to 0 so that the data obtained from the models are similar to the experimental data, even the adjustment is really different for each isotherm model (as can be seen in Table 3). The Freundlich model was preferentially fitted to the data for both Cd(II) adsorption isotherms, SB and BB (R^2 0.981 and 0.956, respectively). The Freundlich equilibrium constant (K_F) was higher for pine sawdust biochar (SB) than for barley char (BB), according to the data provided in Table 3. The Freundlich intensity parameter (*n*) [29] suggested that both biochars adsorb favorably ($0 < 1/n < 1$). As mentioned previously by Wang et al., 2020 [49], when using poplar wood biochar, in their case, the Freundlich model with an R^2 of 0.99 could also describe the adsorption of cadmium ions. Similarly, for Cd(II) adsorption on rice straw biochar and banana biochar, the Freundlich model fit slightly better than the Langmuir model [56,57]. In addition, Hamzenejad et al., 2020 [53] reported the Freundlich model to be the best-performing model for describing Cd(II) adsorption on biochars produced from apple and grape pruning residues. This was in contrast to the results of Cheng et al. 2021 [38], who found that the Langmuir model better fits cadmium adsorption either on willow-derived biochar or poplar sawdust biochar.

Table 3. Cd(II) adsorption parameters determined from the Langmuir and Freundlich isotherm models on SB and BB.

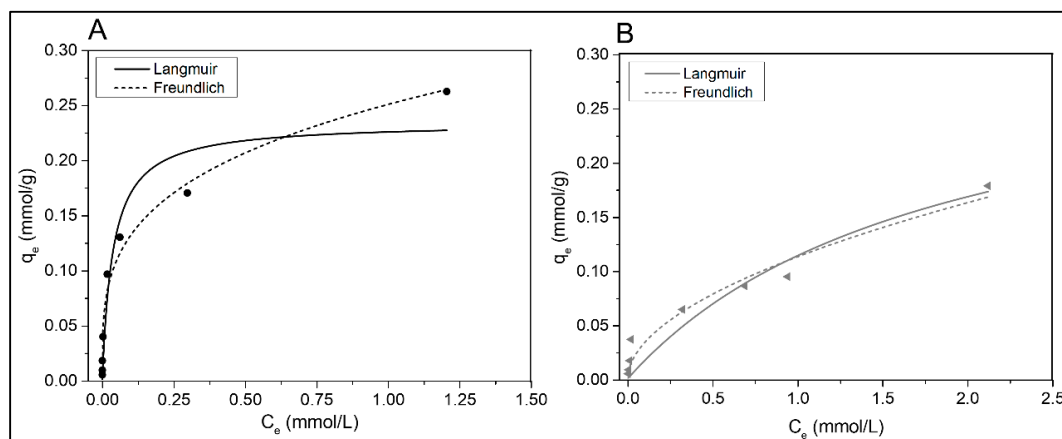| Adsorbent	Langmuir			Freundlich		
	R^2	q_m (mmol/g)	K_L (L/mmol)	R^2	*n*	K_F (mmol$^{1-(1/n)}$ L$^{1/n}$ g^{-1})
SB	0.914	0.23 ± 0.02	26 ± 12	0.981	3.6 ± 0.30	0.25 ± 0.010
BB	0.910	0.30 ± 0.10	0.50 ± 0.30	0.956	1.9 ± 0.30	0.11 ± 0.0060

Figure 8. Cd(II) adsorption isotherms in single-metal systems on (**A**) SB and (**B**) BB.

The parameters derived from the Langmuir isotherm model are also summarized in Table 3. Both residues have similar saturated monolayer adsorption capacity of the adsorbent (q_m). Because the affinity for metal ions is substantially higher in SB, as K_L results, this residue can be considered better than BB for this metal system. A good adsorbent has high q_m and K_L values, according to Tran et al., 2017 [29]. For the range of initial concentrations evaluated, the R_L values were 0.96–0.25 for sawdust char and 0.99–0.45 for barley char. As a result, the adsorption nature was favorable for both adsorbents ($0 < R_L < 1$), although SB as a cadmium adsorbent is more efficient than BB, and the isotherm had a concave shape.

For comparison, some results reported in the literature for q_m for Cd(II) adsorption on different wastes are summarized in Table 4. Although the experimental conditions of each adsorption test were different, it can be confirmed that the sawdust and barley biochars tested here gave quite good results in the removal of Cd(II) ions.

Table 4. Comparison of the maximum adsorption capacity (q_m) of several biochars for the adsorption of cadmium from aqueous solutions.

Adsorbent	Test Conditions	q_m (mg/g)	Ref.
Sawdust biochar (SB) Barley biochar (BB)	Adsorbent weight: 0.1 g, solution volume: 10 mL, Cd(II) initial concentration: 6–450 mg/L, pH: 4–5, stirring speed: 40 rpm, time: 24 h, temperature: room temperature	25.8 33.6	This paper
Poplar sawdust biochar	Adsorbent weight: 0.1 g, solution volume: 100 mL, Cd(II) initial concentration: 180–350 mg/L, pH: 5, stirring speed: 300 rpm, time: 24 h, temperature: room temperature	49.3	[37]
Willow wood biochar Cattle manure biochar	Adsorbent weight: 0.05 g, solution volume: 20 mL, Cd(II) initial concentration: 0.05–160 mg/L, time: 24 h, temperature: room temperature	35.2 31.3	[49]
Pine residue biochar	Adsorbent weight: 0.05 g, solution volume: 25 mL, Cd(II) initial concentration: 2.5–360 mg/L, pH: 6, stirring speed: 4000 rpm, time: 24 h, temperature: room temperature	85.5	[58]
Banana biochar	Adsorbent weight: 0.4 g, solution volume: 50 mL, Cd(II) initial concentration: 10–200 mg/L, pH: 5.5, stirring speed: 180 rpm, time: 8 h, temperature: room temperature	32.0	[56]
Grape pruning biochar Apple pruning biochar	Adsorbent weight: 0.05 g, solution volume: 25 mL, Cd(II) initial concentration: 10–200 mg/L, pH: 5, stirring speed: 60 rpm, time: 2 h, temperature: room temperature	57.0 49.0	[53]
Palm oil mill sludge biochar	Adsorbent weight: 0.02 g, solution volume: 100 mL, Cd(II) initial concentration: 10–200 mg/L pH: 10, stirring speed: 150 rpm, time: 240 min, temperature: room temperature	46.2	[59]

3.3. Clean Disposal of Spent Biochars

A good adsorbent must have the ability to be easily regenerated throughout several application cycles using techno-economic approaches. The removal of heavy metals from biochar, however, may become less effective with each application cycle due to mineral loss and pore structure degradation [37]. Despite the abundance of recent articles on the use and suitability of agro-industrial wastes as adsorbents for various heavy metals, the authors of most of these studies do not focus on the regeneration, environmental stability, or eventual disposal of the spent adsorbents, which are critical for their industrial application [4]. Knowing the destiny of the adsorbent/contaminant system is extremely important since it gives a more complete representation of the adsorbent's potential.

The recovery of biomass or biochar adsorbents and their possible reuse in building bricks could be considered as a viable alternative to safe disposal. The manufacture of fired clay bricks from spent agro-industrial adsorbent has been precisely and thoroughly documented in previous studies [37,38]. The incorporation of these lignocellulosic wastes increased the porosity of the bricks and reduced their mechanical performance, the bricks were nevertheless acceptable within Argentine standards as building bricks.

Leaching phenomena correspond to the transfer of contaminants from a stable matrix to a liquid medium, such as water. In this work, leaching tests were performed on bricks made from sawdust biochar (SB), used as an adsorbent for Ni(II), Zn(II), and Cd(II) mixtures. The concentrations of heavy metals in the brick leachates were Ni(II) < 0.05 mg/L, Zn(II) < 0.02 mg/L, and Cd(II) < 0.05 mg/L lower than the maximum concentrations allowed according to Decree No. 2020 of 2007 of Law No. 2214 of the City of Buenos Aires (CABA) [60]. The retention efficiency of bricks containing spent SB is shown in Table 5. The high retention values obtained (above 90%) imply a high degree of effectiveness of the spent sawdust biochar stabilization process. According to the literature [61–63], the generation of stable phases at ceramic firing temperatures could explain the stabilization of the residues and the consequent decrease in the release of trapped heavy metals.

Table 5. Heavy metal retention efficiencies of bricks prepared from spent SB.

Clay Bricks	Retention Efficiency (%)		
	Ni(II)	**Zn(II)**	**Cd(II)**
SB multimetal	>97.3	>99.2	>98.6

4. Conclusions

The most significant physicochemical characteristics of two biochars, sawdust biochar (SB) and barley biochar (BB), were identified. The results were interpreted to correlate with their effectiveness as adsorbents for Cd(II) and two additional heavy metals, Ni(II) and Zn(II). Both SB and BB showed substantial Cd(II) adsorption in 0.18 mmol/L aqueous solution. However, this study's results indicate that the feedstock and conditions for biochar production are crucial for increasing heavy metal adsorption.

The heavy metals' initial concentration influenced their adsorption. The adsorption percentage decreased and the adsorption capacity increased as the initial concentration of the aqueous multimetal solution increased (range from 0.05 to 4 mmol/L), tending to achieve a plateau because of the saturation of the adsorbate active sites. The presence of limited adsorption sites on the residues was demonstrated by comparing adsorption on BB of Cd(II) alone to its adsorption when present in a multielement solution, which decreased as the initial concentration of adsorbates in the mixture increased.

The Freundlich model (multilayer and heterogeneous adsorption) is appropriate for the Cd(II) adsorption isotherm data in both biochars. The capacity of sawdust char as a cadmium adsorbent was higher than that of barley char. Similar results have been reported in the literature. After adsorption, SEM-EDS and XRF confirmed the presence of Cd(II) in both biochars.

After being used as adsorbents, spent biochars could become secondary pollutants if not properly treated or disposed of. Incorporation of spent SB in the preparation of fired clay bricks may be an excellent option for their safe disposal. Consequently, the results presented here may help address concerns about heavy metal leaching arising from the use and disposal of bricks containing spent SBs.

References

1. Saraeian, A.; Hadi, A.; Raji, F.; Ghassemi, A.; Johnson, M. Cadmium Removal from Aqueous Solution by Low-Cost Native and Surface Modified Sorghum × Drummondii (Sudangrass). *J. Environ. Chem. Eng.* **2018**, *6*, 3322–3331. [CrossRef]
2. Kubier, A.; Wilkin, R.T.; Pichler, T. Cadmium in Soils and Groundwater: A Review. *Appl. Geochem.* **2019**, *108*, 104388. [CrossRef] [PubMed]
3. Zhang, H.; Reynolds, M. Cadmium Exposure in Living Organisms: A Short Review. *Sci. Total Environ.* **2019**, *678*, 761–767. [CrossRef] [PubMed]
4. Othmani, A.; Magdouli, S.; Senthil Kumar, P.; Kapoor, A.; Chellam, P.V.; Gökkuş, Ö. Agricultural Waste Materials for Adsorptive Removal of Phenols, Chromium (VI) and Cadmium (II) from Wastewater: A Review. *Environ. Res.* **2022**, *204*, 111916. [CrossRef]
5. Genchi, G.; Sinicropi, M.S.; Lauria, G.; Carocci, A.; Catalano, A. The Effects of Cadmium Toxicity. *Int. J. Environ. Res. Public Health* **2020**, *17*, 3782. [CrossRef] [PubMed]
6. Kumar, A.; Subrahmanyam, G.; Mondal, R.; Cabral-Pinto, M.M.S.; Shabnam, A.A.; Jigyasu, D.K.; Malyan, S.K.; Fagodiya, R.K.; Khan, S.A.; Yu, Z.G. Bio-Remediation Approaches for Alleviation of Cadmium Contamination in Natural Resources. *Chemosphere* **2021**, *268*, 128855. [CrossRef] [PubMed]
7. United States Environmental Protection Agency (USEPA). *National Primary Drinking Water Regulations*; USEPA: Washington, DC, USA, 2019.
8. Código Alimentario Argentino (CAA) Capítulo XII: Bebidas Analcohólicas. Bebidas Hídricas, Agua y Agua Gasificada. Agua Potable. Argentinian Law (18284), Regulated by Decreto 2126/1971, Art 982. 2012. Available online: https://alimentosargentinos.magyp.gob.ar/contenido/marco/CAA/capitulospdf/Capitulo_XII.pdf (accessed on 27 June 2024).
9. Kwikima, M.M.; Mateso, S.; Chebude, Y. Potentials of Agricultural Wastes as the Ultimate Alternative Adsorbent for Cadmium Removal from Wastewater. *A Rev. Sci. Afr.* **2021**, *13*, e00934. [CrossRef]
10. Vardhan, K.H.; Kumar, P.S.; Panda, R.C. A Review on Heavy Metal Pollution, Toxicity and Remedial Measures: Current Trends and Future Perspectives. *J. Mol. Liq.* **2019**, *290*, 111197. [CrossRef]
11. Sahu, S.; Pandey, M.; Sharma, S. A Review on Low-Cost Adsorbents for Cadmium Pollutant Removal from Industrial Effluents. *Adv. Mater. Lett.* **2021**, *5*, 21051627. [CrossRef]
12. Pyrzynska, K. Removal of Cadmium from Wastewaters with Low-Cost Adsorbents. *J. Environ. Chem. Eng.* **2019**, *7*, 102795. [CrossRef]
13. Acharya, J.; Kumar, U.; Rafi, P.M. Removal of Heavy Metal Ions from Wastewater by Chemically Modified Agricultural Waste Material as Potential Adsorbent—A Review. *Int. J. Curr. Eng. Technol.* **2018**, *8*, 526–530. [CrossRef]
14. Yousef, R.; Qiblawey, H.; El-Naas, M.H. Adsorption as a Process for Produced Water Treatment: A Review. *Processes* **2020**, *8*, 1657. [CrossRef]
15. Deshmukh, P.D.; Khadse, G.K.; Shinde, V.M.; Labhasetwar, P. Cadmium Removal from Queous Solutions Using Dried Banana Peels as an Adsorbent: Kinetics and Equilibrium Modeling. *J. Bioremediat. Biodegrad.* **2017**, *8*, 1–7. [CrossRef]
16. Basu, M.; Guha, A.K.; Ray, L. Adsorption Behavior of Cadmium on Husk of Lentil. *Process Saf. Environ. Prot.* **2017**, *106*, 11–22. [CrossRef]

17. Abatan, O.G.; Alaba, P.A.; Oni, B.A.; Akpojevwe, K.; Efeovbokhan, V.; Abnisa, F. Performance of Eggshells Powder as an Adsorbent for Adsorption of Hexavalent Chromium and Cadmium from Wastewater. *SN Appl. Sci.* **2020**, *2*, 1996. [CrossRef]

18. Santos, V.H.; do Nascimento, G.E.; Sales, D.C.S.; dos Santos, J.H.L.; Rodríguez-Díaz, J.M.; Duarte, M.M.M.B. Preparation of Adsorbents from Agro-Industrial Wastes and Their Application in the Removal of Cd^{2+} and Pb^{2+} Ions from a Binary Mixture: Evaluation of Ionic Competition. *Chem. Eng. Res. Des.* **2022**, *184*, 152–164. [CrossRef]

19. Torres, E. Biosorption: A Review of the Latest Advances. *Processes* **2020**, *8*, 1584. [CrossRef]

20. Mallarino-Miranda, L.; Venner-Gonzalez, J.; Tejeda-Benitez, L. Heavy Metal Adsorption Using Biocarbón from Agricultural and Agro-Industrial Waste for Decontamination of Soils and Water Sources: A Review. *Chem. Eng. Trans.* **2022**, *92*, 709–714. [CrossRef]

21. Abdel-Fattah, T.M.; Mahmoud, M.E.; Ahmed, S.B.; Huff, M.D.; Lee, J.W.; Kumar, S. Biochar from Woody Biomass for Removing Metal Contaminants and Carbon Sequestration. *J. Ind. Eng. Chem.* **2015**, *22*, 103–109. [CrossRef]

22. Liu, T.; Lawluvy, Y.; Shi, Y.; Ighalo, J.O.; He, Y.; Zhang, Y.; Yap, P.S. Adsorption of Cadmium and Lead from Aqueous Solution Using Modified Biochar: A Review. *J. Environ. Chem. Eng.* **2022**, *10*, 106502. [CrossRef]

23. López, J.E.; Builes, S.; Heredia Salgado, M.A.; Tarelho, L.A.C.; Arroyave, C.; Aristizábal, A.; Chavez, E. Adsorption of Cadmium Using Biochars Produced from Agro-Residues. *J. Phys. Chem. C* **2020**, *124*, 14592–14602. [CrossRef]

24. Ahmad, M.; Upamali Rajapaksha, A.; Eun Lim, J.; Zhang, M.; Bolan, N.; Mohan, D.; Vithanage, M.; Soo Lee, S.; Sik Ok, Y. Biochar as a Sorbent for Contaminant Management in Soil and Water: A Review. *Chemosphere* **2014**, *99*, 19–33. [CrossRef] [PubMed]

25. Zhao, J.; Boada, R.; Cibin, G.; Palet, C. Enhancement of Selective Adsorption of Cr Species via Modification of Pine Biomass. *Sci. Total Environ.* **2020**, *756*, 143816. [CrossRef] [PubMed]

26. Clauser, N.M.; Gutiérrez, M.S.; Felissia, F.E.; Area, M.C.; Vallejos, M.E. Sensitivity Assessment of Value-Added Products and Pellet Production in Alternatives for Softwood Sawdust Valorization. *Biomass Convers. Biorefin.* **2024**, *14*, 6659–6669. [CrossRef]

27. Belmartino, A.; Liseras, N. The Craft Beer Market in Argentina: An Exploratory Study of Local Brewers' and Consumers' Perceptions in Mar Del Plata. *Pap. Appl. Geogr.* **2020**, *6*, 190–203. [CrossRef]

28. Hamdaoui, O. Adsorption of Cu(II) from Aqueous Phase by Cedar Bark. *J. Dispers. Sci. Technol.* **2016**, *38*, 1087–1091. [CrossRef]

29. Tran, H.N.; You, S.-J.; Hosseini-Bandegharaei, A.; Chao, H.-P. Mistakes and Inconsistencies Regarding Adsorption of Contaminants from Aqueous Solutions: A Critical Review. *Water Res.* **2017**, *120*, 88–116. [CrossRef] [PubMed]

30. Yagub, M.T.; Sen, T.K.; Afroze, S.; Ang, H.M. Dye and Its Removal from Aqueous Solution by Adsorption: A Review. *Adv. Colloid Interface Sci.* **2014**, *209*, 172–184. [CrossRef] [PubMed]

31. Chakraborty, R.; Asthana, A.; Singh, A.K.; Jain, B.; Susan, A.B.H. Adsorption of Heavy Metal Ions by Various Low-Cost Adsorbents: A Review. *Int. J. Environ. Anal. Chem.* **2020**, *102*, 342–379. [CrossRef]

32. Nawaz Bhatti, H.; Zaman, Q.; Kausar, A.; Noreen, S.; Iqbal, M.; Bhatti, H.N.; Zaman, Q.; Kausar, A.; Noreen, S.; Iqbal, M.; et al. Efficient Remediation of Zr(IV) Using Citrus Peel Waste Biomass: Kinetic, Equilibrium and Thermodynamic Studies. *Ecol. Eng.* **2016**, *95*, 216–228. [CrossRef]

33. Simón, D.; Gass, S.; Palet, C.; Cristóbal, A. Disposal of Wooden Wastes Used as Heavy Metal Adsorbents as Components of Buildings Bricks. *J. Build. Eng.* **2021**, *40*, 102371. [CrossRef]

34. Simón, D.; Gass, S.; Quaranta, N.; Cristóbal, A. Production of fired clay bricks as a safe removal method for spent adsorbents from sunflower and corn residues. *J. Clean. Prod.* **2023**, *426*, 139138. [CrossRef]

35. United States Environmental Protection Agency (USEPA). *SW-846 Test Method 1311 Toxicity Characteristic Leaching Procedure*; USEPA: Washington, DC, USA, 1992.

36. Yilmaz, O.; Ünlü, K.; Cokca, E. Solidification/Stabilization of Hazardous Wastes Containing Metals and Organic Contaminants. *J. Environ. Eng.* **2003**, *129*, 366–376. [CrossRef]

37. Cheng, S.; Liu, Y.; Xing, B.; Qin, X.; Zhang, C.; Xia, H. Lead and Cadmium Clean Removal from Wastewater by Sustainable Biochar Derived from Poplar Saw Dust. *J. Clean. Prod.* **2021**, *314*, 128074. [CrossRef]

38. Chen, X.; Chen, G.; Chen, L.; Chen, Y.; Lehmann, J.; McBride, M.B.; Hay, A.G. Adsorption of Copper and Zinc by Biochars Produced from Pyrolysis of Hardwood and Corn Straw in Aqueous Solution. *Bioresour. Technol.* **2011**, *102*, 8877–8884. [CrossRef] [PubMed]

39. Elgarahy, A.M.; Elwakeel, K.Z.; Mohammad, S.H.; Elshoubaky, G.A. A Critical Review of Biosorption of Dyes, Heavy Metals and Metalloids from Wastewater as an Efficient and Green Process. *Clean. Eng. Technol.* **2021**, *4*, 100209. [CrossRef]

40. Nguyen, T.H.; Tran, H.N.; Vu, H.A.; Trinh, M.V.; Nguyen, T.V.; Loganathan, P.; Vigneswaran, S.; Nguyen, T.M.; Trinh, V.T.; Vu, D.L.; et al. Laterite as a Low-Cost Adsorbent in a Sustainable Decentralized Filtration System to Remove Arsenic from Groundwater in Vietnam. *Sci. Total Environ.* **2020**, *699*, 134267. [CrossRef] [PubMed]

41. Zhao, J.J.; Shen, X.J.; Domene, X.; Alcañiz, J.M.; Liao, X.; Palet, C. Comparison of Biochars Derived from Different Types of Feedstocks and Their Potential for Heavy Metal Removal in Multiple-Metal Solutions. *Sci. Rep.* **2019**, *9*, 1–12. [CrossRef]

42. Inyang, M.I.; Gao, B.; Yao, Y.; Xue, Y.; Zimmerman, A.; Mosa, A.; Pullammanappallil, P.; Ok, Y.S.; Cao, X. A Review of Biochar as a Low-Cost Adsorbent for Aqueous Heavy Metal Removal. *Crit. Rev. Environ. Sci. Technol.* **2015**, *46*, 406–433. [CrossRef]

43. Otieno, A.O.; Home, P.G.; Raude, J.M.; Murunga, S.I.; Ngumba, E.; Ojwang, D.O.; Tuhkanen, T. Pineapple Peel Biochar and Lateritic Soil as Adsorbents for Recovery of Ammonium Nitrogen from Human Urine. *J. Environ. Manag.* **2021**, *293*, 112794. [CrossRef] [PubMed]

44. Quaranta, N.; Caligaris, M.; Pelozo, G.; Unsen, M.; Cristóbal, A. The Characterization of Brewing Waste and Feasibility of Its Use for the Production of Porous Ceramics. *WIT Trans. Ecol. Environ.* **2016**, *202*, 299–310. [CrossRef]

45. Afroze, S.; Sen, T.K. A Review on Heavy Metal Ions and Dye Adsorption from Water by Agricultural Solid Waste Adsorbents. *Water Air Soil Pollut.* **2018**, *229*, 1–50. [CrossRef]

46. Elhassan, M.; Kooh, M.R.R.; Chou Chau, Y.F.; Abdullah, R. Hydrochar from Shorea spp.: A dual-purpose approach for sustainable biofuel and efficient methylene blue adsorbent. *Biomass Conv. Bioref.* **2024**, 2190–6823. [CrossRef]

47. Amen, R.; Yaseen, M.; Mukhtar, A.; Klemeš, J.J.; Saqib, S.; Ullah, S.; Al-Sehemi, A.G.; Rafiq, S.; Babar, M.; Fatt, C.L.; et al. Lead and Cadmium Removal from Wastewater Using Eco-Friendly Biochar Adsorbent Derived from Rice Husk, Wheat Straw, and Corncob. *Clean. Eng. Technol.* **2020**, *1*, 100006. [CrossRef]

48. Shan, R.; Shi, Y.; Gu, J.; Wang, Y.; Yuan, H. Single and Competitive Adsorption Affinity of Heavy Metals toward Peanut Shell-Derived Biochar and Its Mechanisms in Aqueous Systems. *Chinese J. Chem. Eng.* **2020**, *28*, 1375–1383. [CrossRef]

49. Wang, S.; Kwak, J.H.; Islam, M.S.; Naeth, M.A.; Gamal El-Din, M.; Chang, S.X. Biochar Surface Complexation and Ni(II), Cu(II), and Cd(II) Adsorption in Aqueous Solutions Depend on Feedstock Type. *Sci. Total Environ.* **2020**, *712*, 136538. [CrossRef] [PubMed]

50. Petrella, A.; Spasiano, D.; Acquafredda, P.; De Vietro, N.; Ranieri, E.; Cosma, P.; Rizzi, V.; Petruzzelli, V.; Petruzzelli, D. Heavy Metals Retention (Pb(II), Cd(II), Ni(II)) from Single and Multimetal Solutions by Natural Biosorbents from the Olive Oil Milling Operations. *Process Saf. Environ. Prot.* **2018**, *114*, 79–90. [CrossRef]

51. Romano, M.S.; Corne, V.; Azario, R.R.; García, M.C. Aprovechamiento de Residuos Lignocelulósicos Regionales Para La Remoción de Cadmio En Solución. *Av. En Cienc. E Ing.* **2020**, *11*, 11–22.

52. Sobhanardakani, S.; Parvizimosaed, H.; Olyaie, E. Heavy Metals Removal from Wastewaters Using Organic Solid Waste-Rice Husk. *Environ. Sci. Pollut. Res.* **2013**, *20*, 5265–5271. [CrossRef] [PubMed]

53. Hamzenejad Taghlidabad, R.; Sepehr, E.; Khodaverdiloo, H.; Samadi, A.; Rasouli-Sadaghiani, M.H. Characterization of Cadmium Adsorption on Two Cost-Effective Biochars for Water Treatment. *Arab. J. Geosci.* **2020**, *13*, 448. [CrossRef]

54. Semerjian, L. Removal of Heavy Metals (Cu, Pb) from Aqueous Solutions Using Pine (Pinus Halepensis) Sawdust: Equilibrium, Kinetic, and Thermodynamic Studies. *Environ. Technol. Innov.* **2018**, *12*, 91–103. [CrossRef]

55. Njoku, V.O. Biosorption Potential of Cocoa Pod Husk for the Removal of Zn(II) from Aqueous Phase. *J. Environ. Chem. Eng.* **2014**, *2*, 881–887. [CrossRef]

56. Liu, X.; Li, G.; Chen, C.; Zhang, X.; Zhou, K.; Long, X. Banana Stem and Leaf Biochar as an Effective Adsorbent for Cadmium and Lead in Aqueous Solution. *Sci. Rep.* **2022**, *12*, 1–14. [CrossRef]

57. Deng, Y.; Huang, S.; Dong, C.; Meng, Z.; Wang, X. Competitive Adsorption Behaviour and Mechanisms of Cadmium, Nickel and Ammonium from Aqueous Solution by Fresh and Ageing Rice Straw Biochars. *Bioresour. Technol.* **2020**, *303*, 122853. [CrossRef] [PubMed]

58. Park, J.H.; Wang, J.J.; Kim, S.H.; Kang, S.W.; Jeong, C.Y.; Jeon, J.R.; Park, K.H.; Cho, J.S.; Delaune, R.D.; Seo, D.C. Cadmium Adsorption Characteristics of Biochars Derived Using Various Pine Tree Residues and Pyrolysis Temperatures. *J. Colloid Interface Sci.* **2019**, *553*, 298–307. [CrossRef] [PubMed]

59. Goh, C.L.; Sethupathi, S.; Bashir, M.J.; Ahmed, W. Adsorptive Behaviour of Palm Oil Mill Sludge Biochar Pyrolyzed at Low Temperature for Copper and Cadmium Removal. *J. Environ. Manag.* **2019**, *237*, 281–288. [CrossRef] [PubMed]

60. Decreto 2020/2007 Reglamentación Ley 2214. Residuos Peligrosos de La Ciudad de Buenos Aires. Concepto. Generación. Regulación. Manipulación. Transporte. Disposición Final. Publication in 13/12/2007. 2007. Available online: https://boletinoficial.buenosaires.gob.ar/normativaba/norma/111841 (accessed on 27 June 2024).

61. Kurmus, H.; Mohajerani, A. Leachate Analysis of Heavy Metals in Cigarette Butts and Bricks Incorporated with Cigarette Butts. *Materials* **2020**, *13*, 2843. [CrossRef] [PubMed]

62. Yaras, A.; Sutcu, M.; Erdogmus, E.; Gencel, O. Recycling and Immobilization of Zinc Extraction Residue in Clay-Based Brick Manufacturing. *J. Build. Eng.* **2021**, *41*, 102421. [CrossRef]

63. Simón, D.; Palet, C.; Costas, A.; Cristóbal, A. Agro-Industrial Waste as Potential Heavy Metal Adsorbents and Subsequent Safe Disposal of Spent Adsorbents. *Water* **2022**, *14*, 3298. [CrossRef]